

Supplementary Information

Revealing Practical Specific Capacity and Carbonyl Utilization of Multi-carbonyl Compounds for Organic Cathode Materials

Jun-Lin Shi^a, Shi-Qin Xiang^a, Dai-Jian Su^a, Rongxing He^a, and Liu-Bin Zhao^{a,*}

^aDepartment of Chemistry, School of Chemistry and Chemical Engineering, Southwest University, Chongqing, 400715, China

Corresponding Author

*E-mail: lbzhao@swu.edu.cn

Table S1. Abbreviations and full names of studied multi-carbonyl compounds in this work.

Abbreviations	Full names
PT	pentacene-5,7,12,14-tetraone
PTO	pyrene-4,5,9,10-tetraone
PMDA	1,3,4,6-pyromellitic dianhydride
NTCDA	1,4,5,8-naphthalenetetracarboxylic dianhydride
PMDI	1,3,4,6-pyromellitic diimide
NTCDI	1,4,5,8-naphthalenetetracarboxylic diimide
α -HAHA	heptacene-5,7,9,14,16,18-hexaone
β -HAHA	heptacene-6,7,8,15,16,17-hexaone
α -HAOA	heptacen-1,4,6,8,10,13,15,17-octaone
β -HAOA	heptacen-5,6,8,9,14,15,17,18-octaone
α -HADA	heptacene-1,4,6,7,8,10,13,15,16,17-decaone
β -HADA	heptacene-5,6,7,8,9,14,15,16,17,18-decaone
TPHA	triphenylene-2,3,6,7,10,11-hexaone
TTOA	tribenzo[f,k,m]tetraphen-2,3,6,7,11,12,15,16-octaone
CCDA	circumcoronene-2,3,5,6,8,9,11,12,14,15,17,18-dodecaone
TQA	triquinoxalinylene

Table S2. Summary of Electrochemical Performance Including Average Discharge Potential (V vs. Li⁺/Li), Specific Capacity (mAh·g⁻¹), and Energy Density (Wh·kg⁻¹) of Studied Multi-carbonyl Compounds.

Molecule	Molecule Weight	Average Discharge Potential	Specific Capacity	Energy Density
PT	338	2.09	317	655
PTO	262	2.50	409	1012
PMDA	218	1.51	492	732
PMDI	216	1.32	496	644
NTCDA	268	1.79	400	702
NTCDI	266	1.48	403	587
α -HAHA	468	2.05	342	702
β -HAHA	468	2.40	342	819
α -HAOA	498	2.19	430	942
β -HАОA	498	2.33	430	1003
α -HADA	528	2.38	507	1205
β -HADA	528	2.51	507	1274
TPHA	318	2.97	505	1502
TTOA	498	2.93	478	1401
CCDA	847	2.52	380	956
TQA	384	1.57	418	657

Table S3. The optimized geometries and calculated thermal free energies (in a.u.) of PT, PTO, PMDA, NTCDA, PMDI, and NTCDI in each lithiation state.

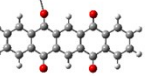
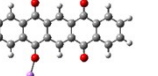
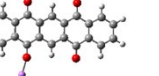
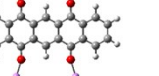
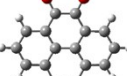
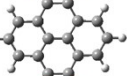
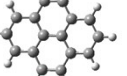
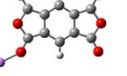
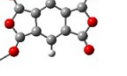
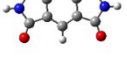
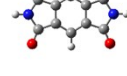
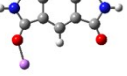
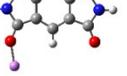
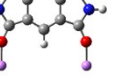
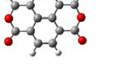
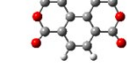
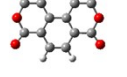
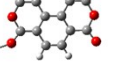
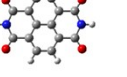
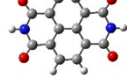
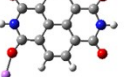
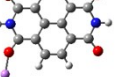
	Li_0	Li_1	Li_2	Li_3	Li_4
PT					
	-1145.396	-1153.040	-1160.667	-1168.274	-1175.872
PTO					
	-914.328	-921.987	-929.622	-937.255	-944.865
PMDA					
	-833.828	-841.473	-849.095	-856.672	-864.219
PMDI					
	-794.084	-801.717	-809.332	-816.897	-824.447
NTCDA					
	-987.472	-995.121	-1002.753	-1010.335	-1017.903
NTCDI					
	-947.738	-955.380	-963.005	-970.571	-978.125

Table S4. Calculated lithiation potentials of PT (V vs. Li⁺/Li) by using different theoretical methods.

	E ₁	E ₂	E ₃	E ₄	E _{ave}
GGA-PBE ^a	1.26	2.04	0.96	0.84	1.27
DFT-D2 ^a	1.97	1.86	1.62	1.74	1.80
DFT-D3 ^a	1.31	1.49	1.46	0.99	1.31
B3LYP ^b	2.77	2.29	1.78	1.51	2.09
Exp. ^c	2.6	2.3	1.8		2.1

^a Periodic DFT calculations with projected-augmented wave (PAW)¹ approach by using the VASP (Vienna Ab initio Simulation Package) code^{2,3}.

^b Single molecule model at PCM/B3LYP/6-311+G(d,p)⁴⁻⁷ level by using the Gaussian 09 program⁸.

^c Data from Ref^{9,10}.

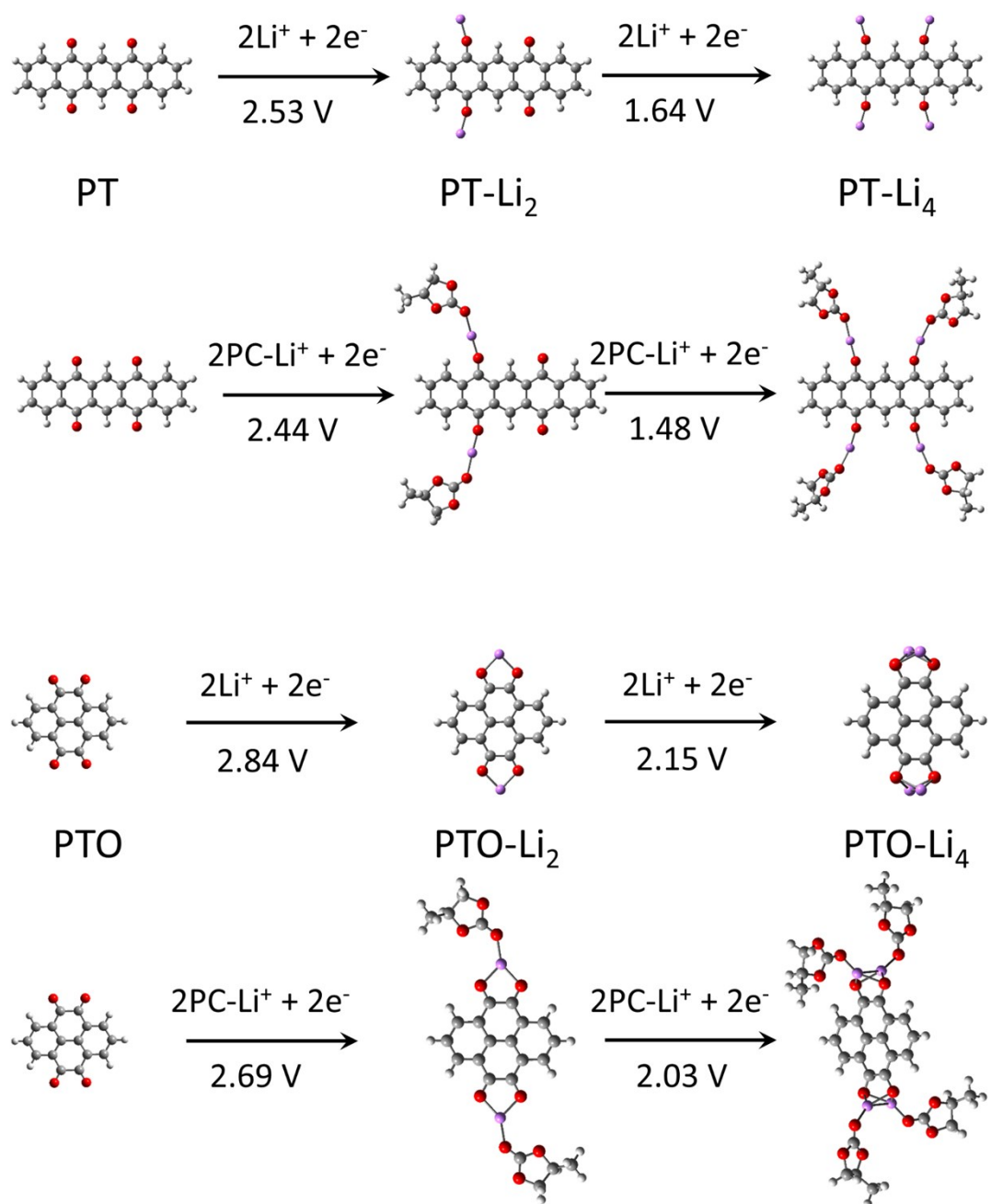


Figure S1. Comparison of discharge potentials of PT and PTO calculated by implicit solvation model and hybrid implicit-explicit solvation model.

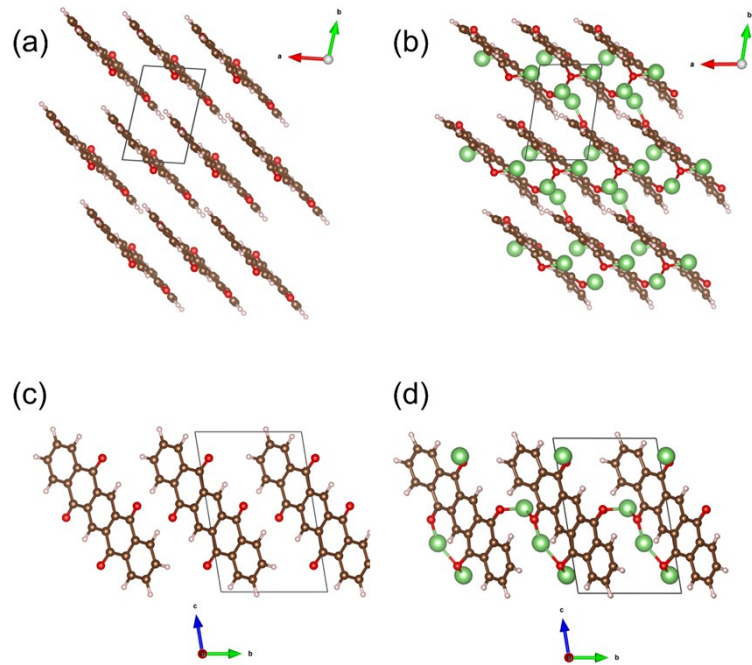


Figure S2. Crystal structure of PT in fully-charged state viewed from (a) the *c* direction and (c) the *a* direction. Crystal structure of PT in fully-discharged state from (b) the *c* direction and (d) the *a* direction.

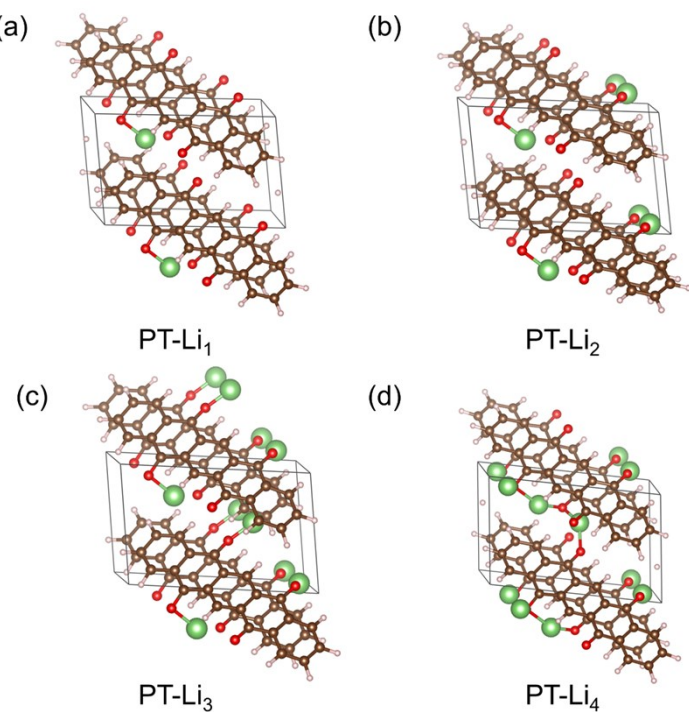


Figure S3. Crystal structure of PT in different discharged stages (a) PT-Li₁, (b) PT-Li₂, (c) PT-Li₃, (d) PT-Li₄.

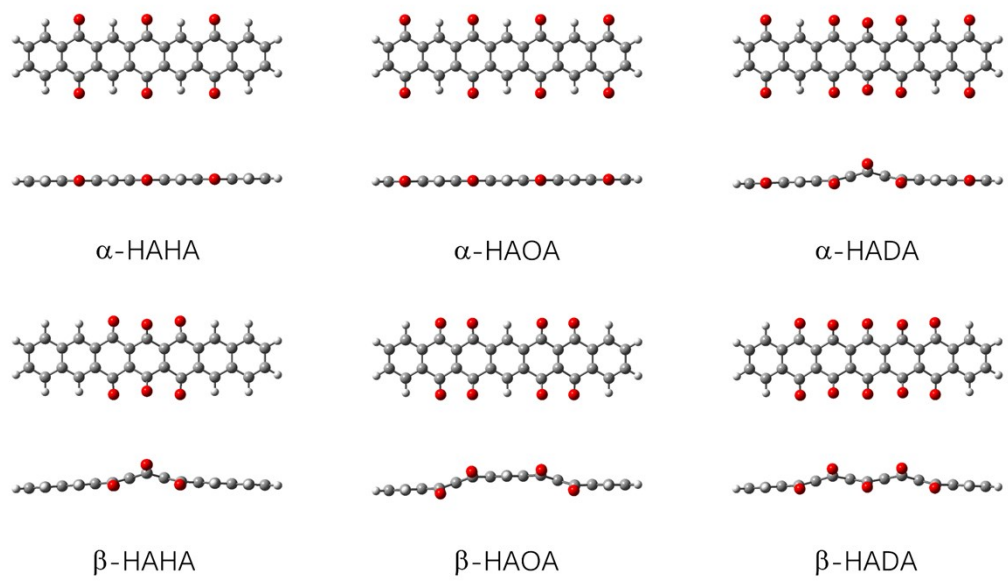


Figure S4. Top views and side views of a series conjugated multi-carbonyl groups based on heptacene prototype with para-dicarbonyl fragments.

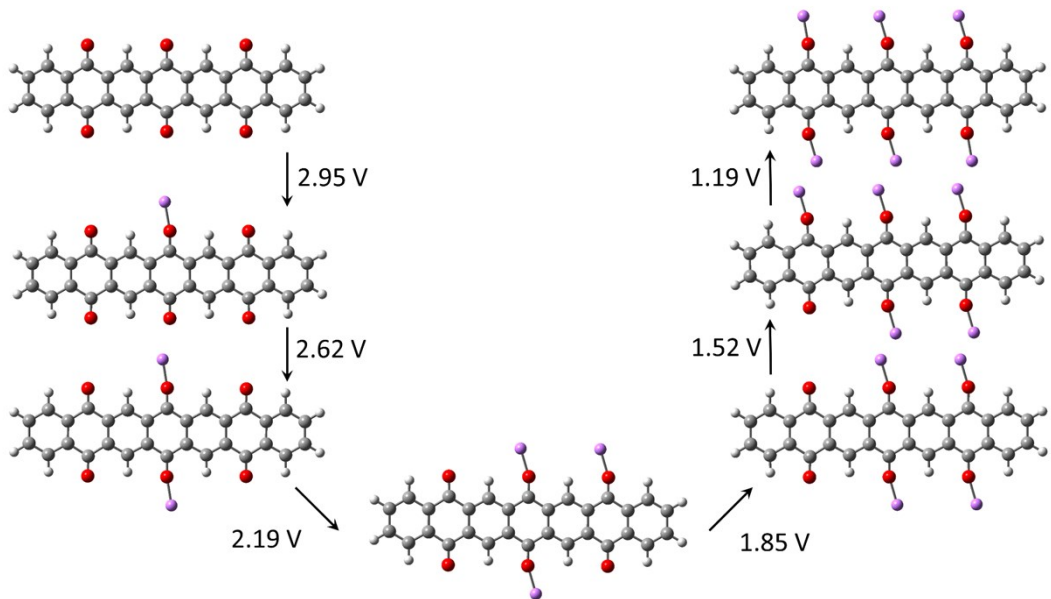


Figure S5. Structure evolution of α -HAHA during elementary lithiation processes.

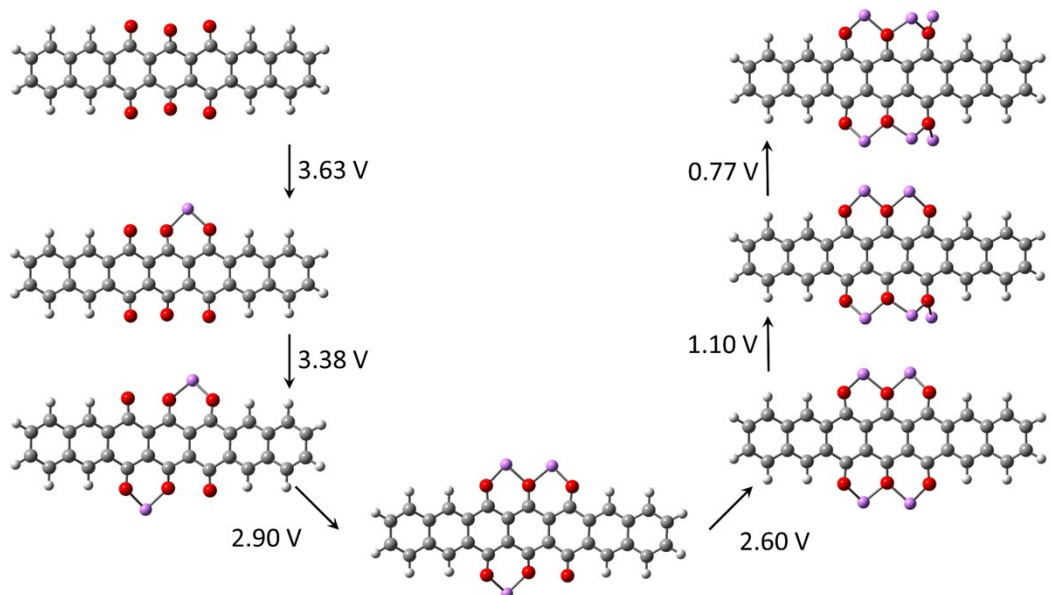


Figure S6. Structure evolution of β -HAHA during elementary lithiation processes.

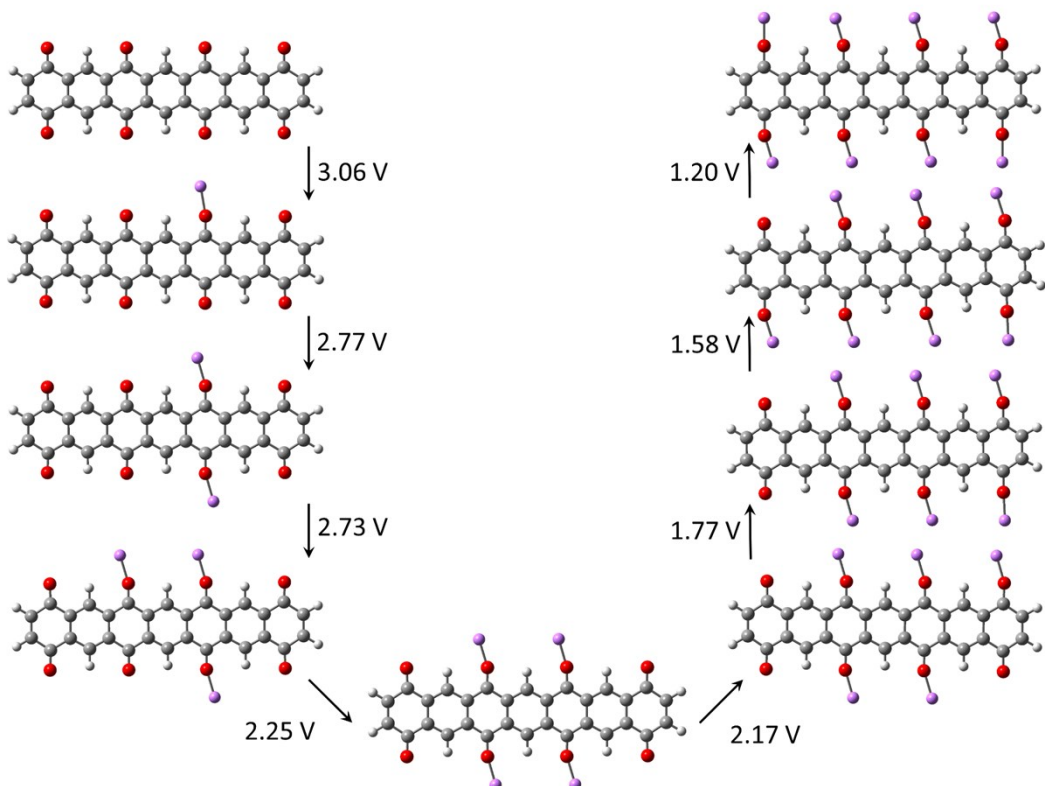


Figure S7. Structure evolution of α -HAOA during elementary lithiation processes.

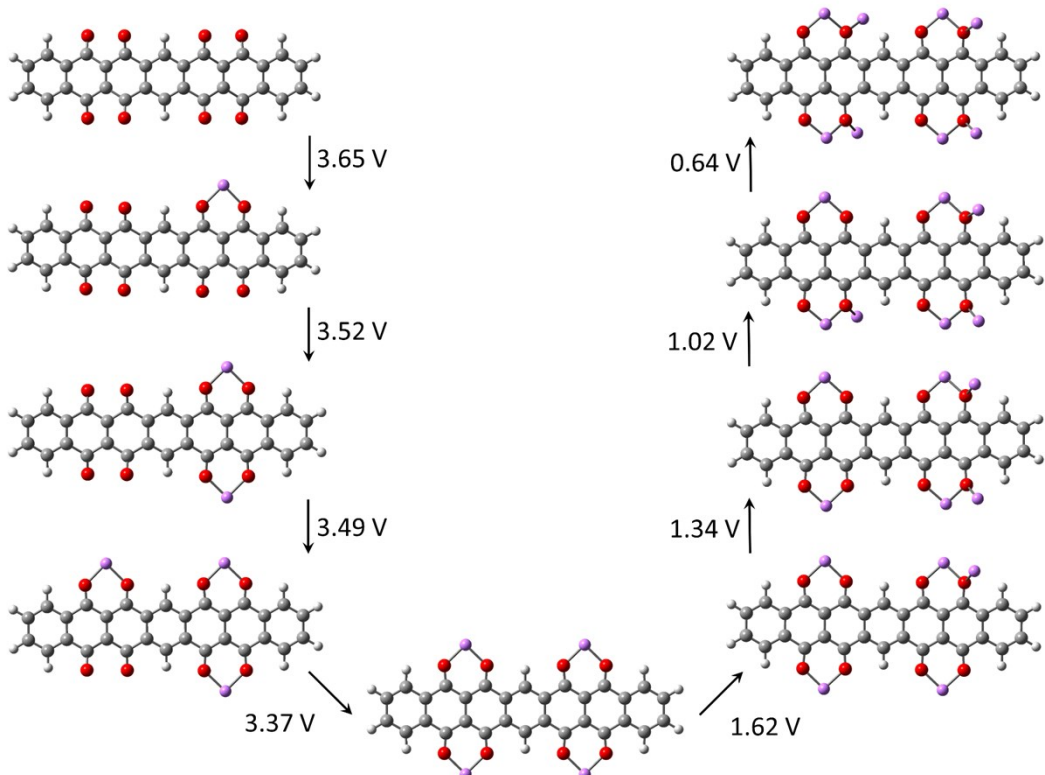


Figure S8. Structure evolution of β -HAOA during elementary lithiation processes.

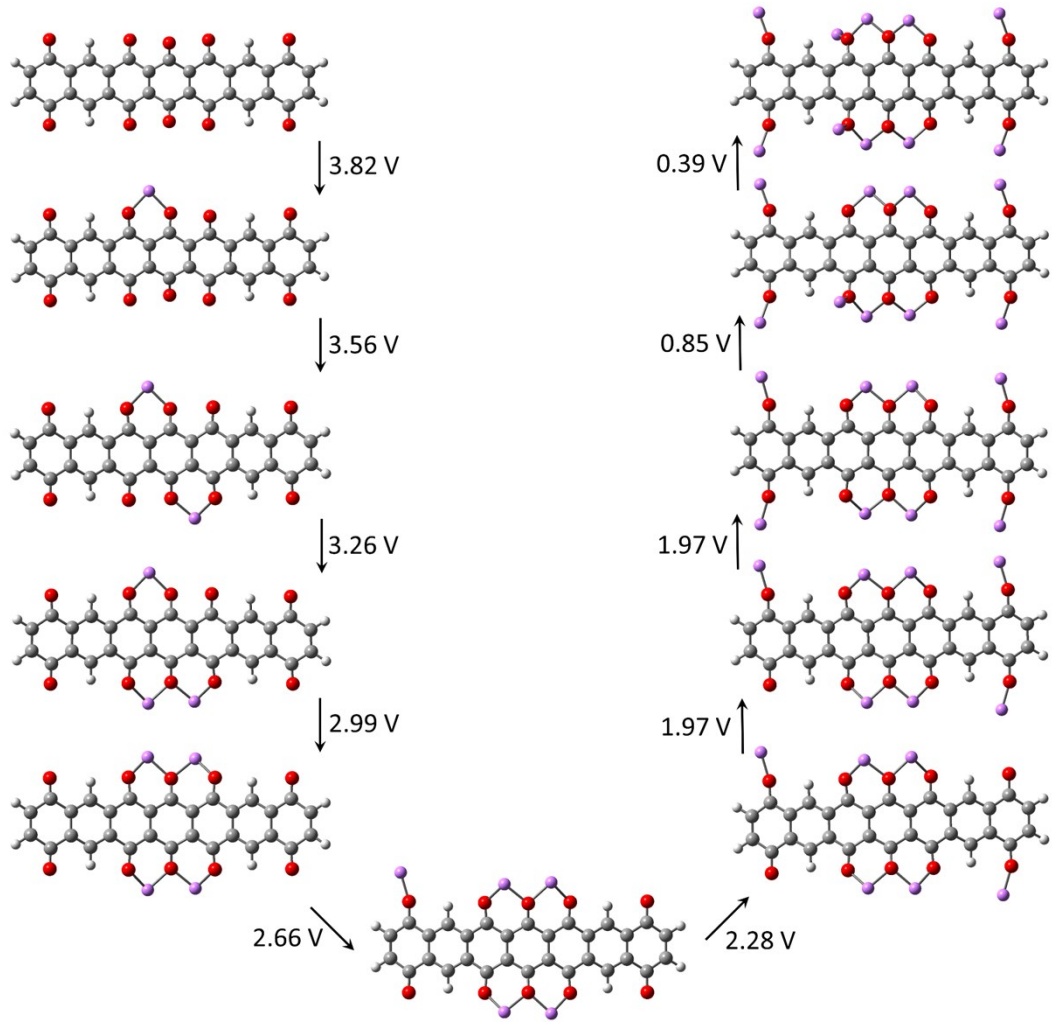


Figure S9. Structure evolution of α -HADA during elementary lithiation processes.

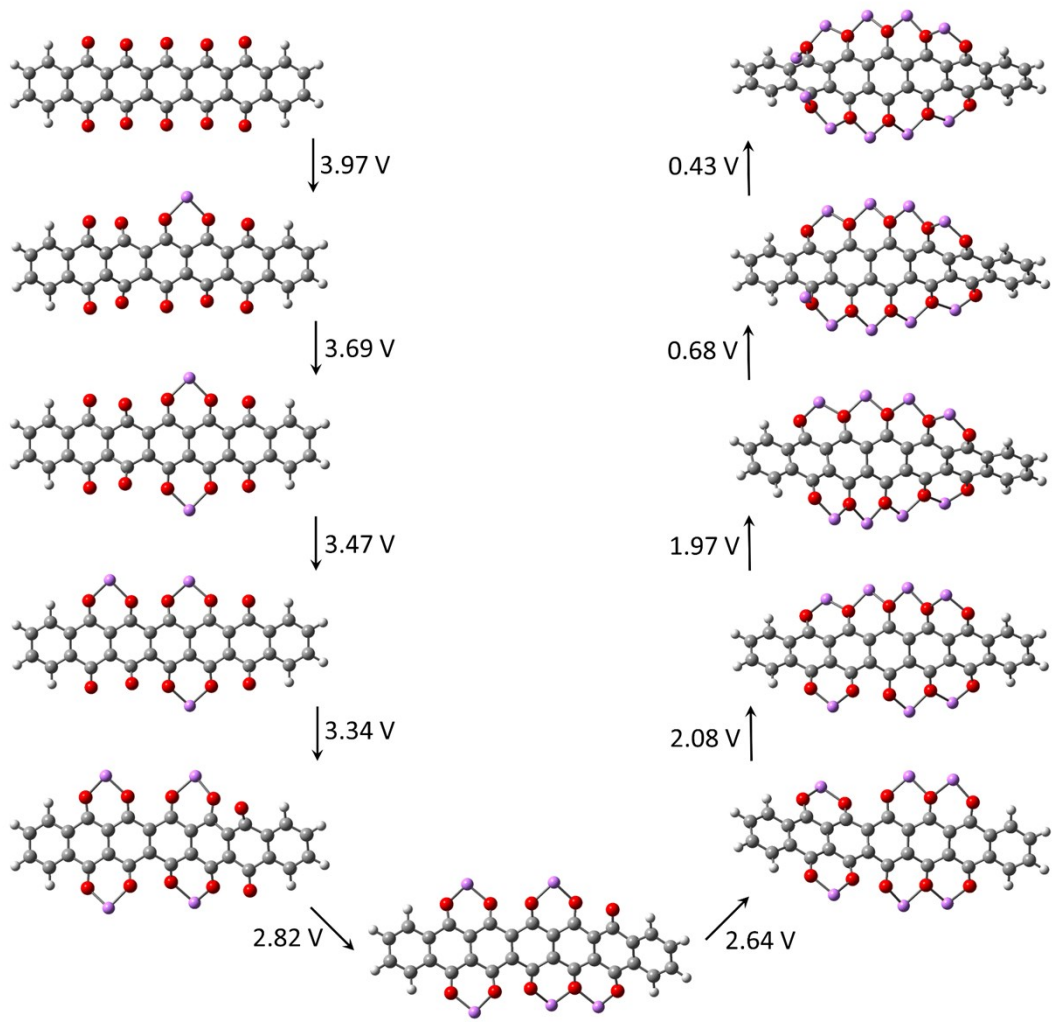


Figure S10. Structure evolution of β -HADA during elementary lithiation processes.

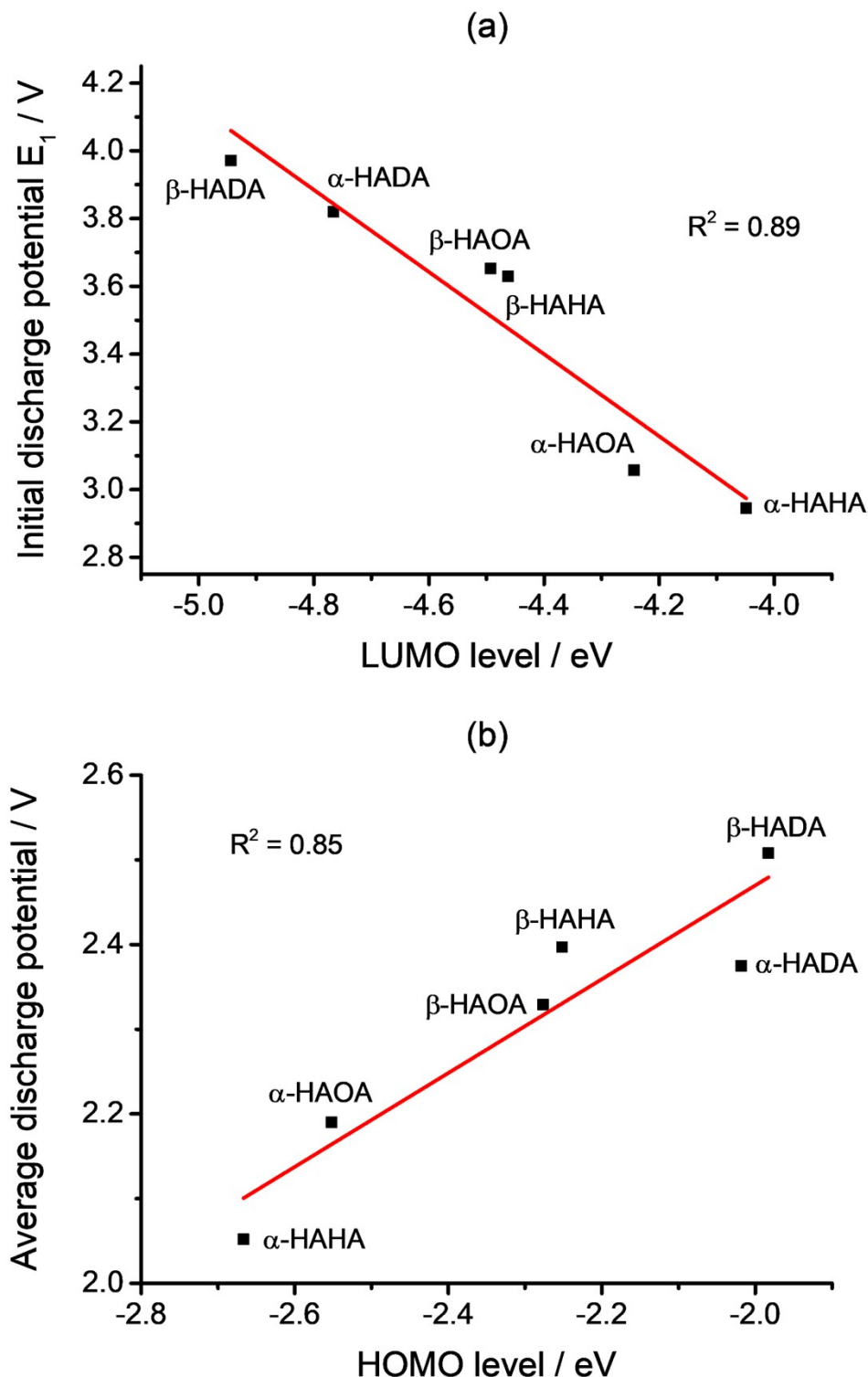


Figure S11. (a) Linear relationship of first lithiation potentials and LUMO levels of organic molecules in charged state and (b) linear relationship of average discharge potential and HOMO levels of organic molecules in discharged state.

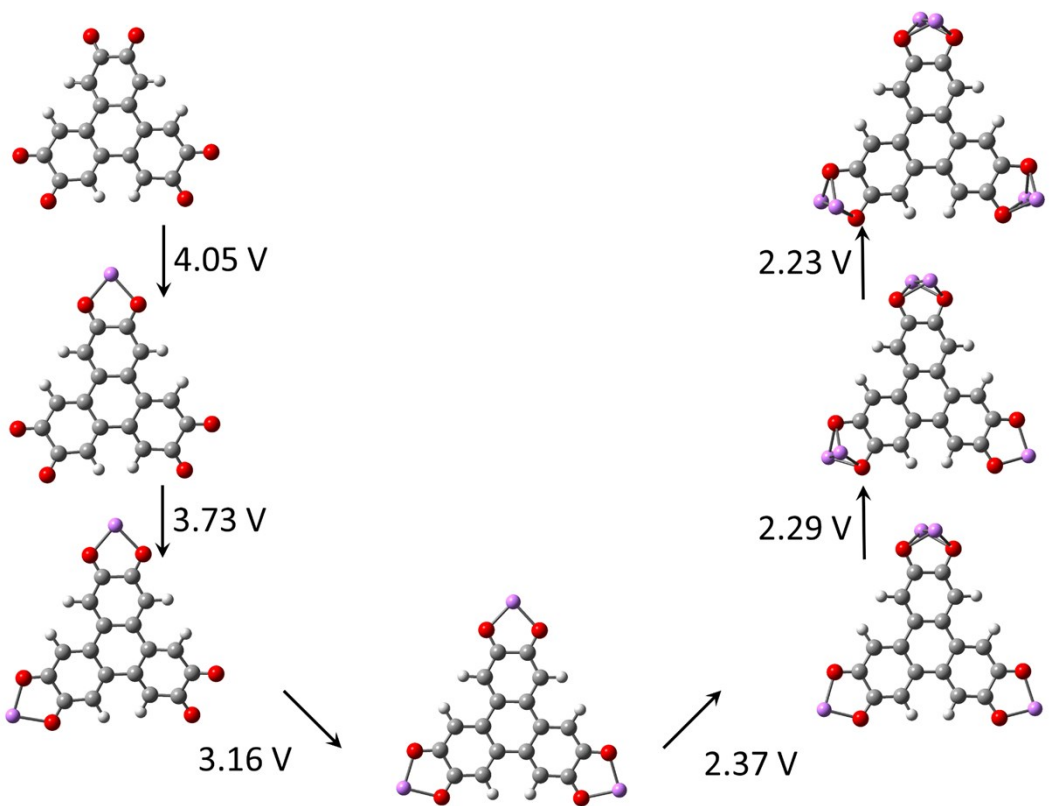


Figure S12. Structure evolution of TPHA during elementary lithiation processes.

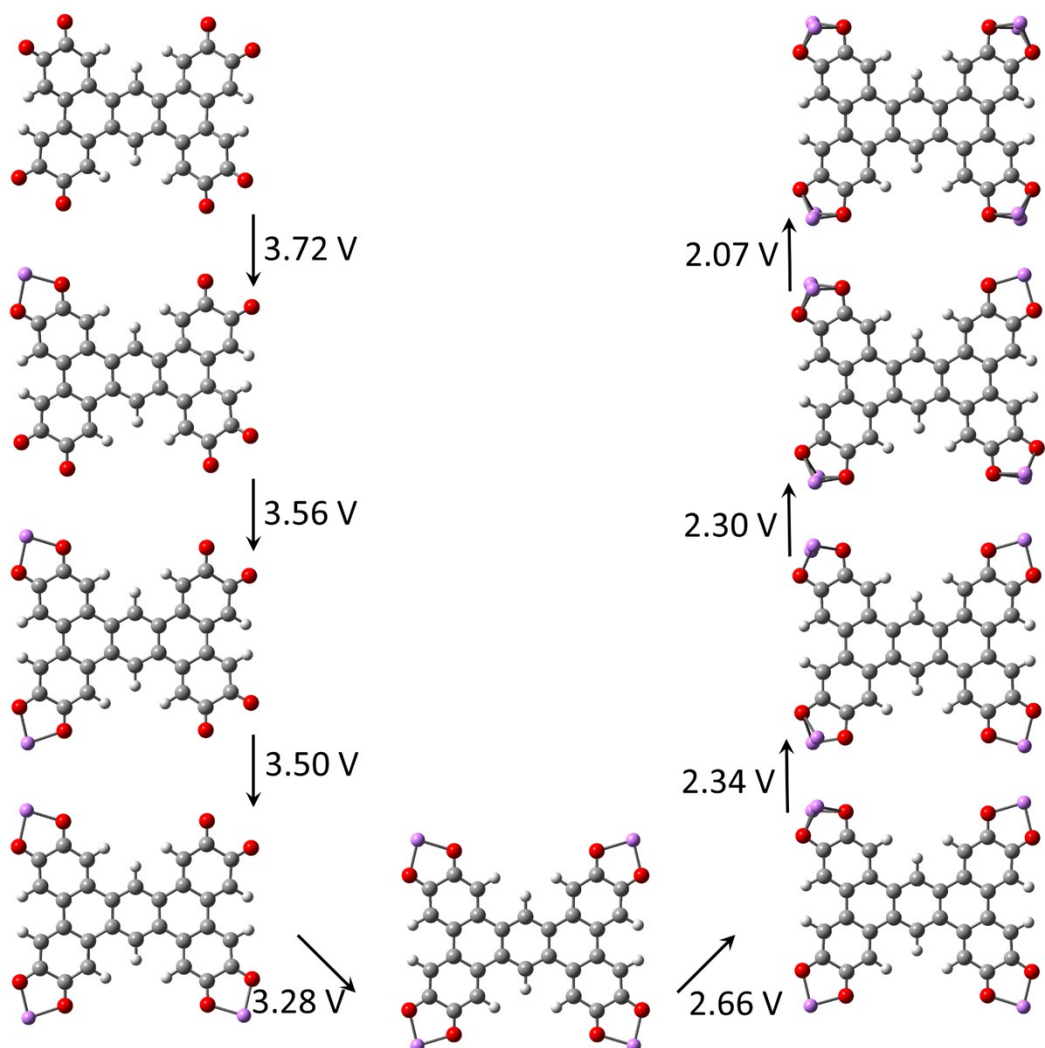


Figure S13. Structure evolution of TTOA during elementary lithiation processes.

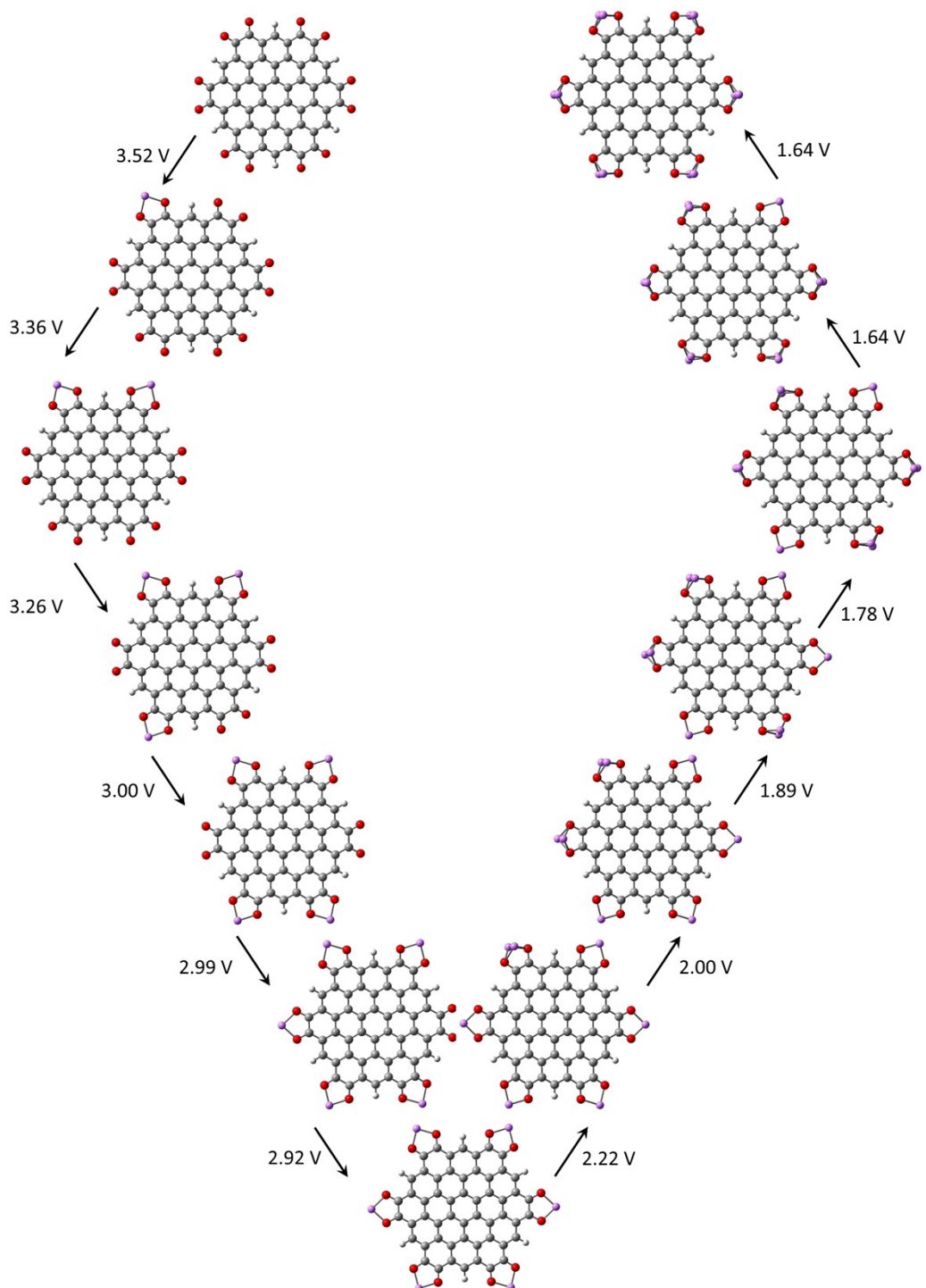


Figure S14. Structure evolution of CCDA during elementary lithiation processes.

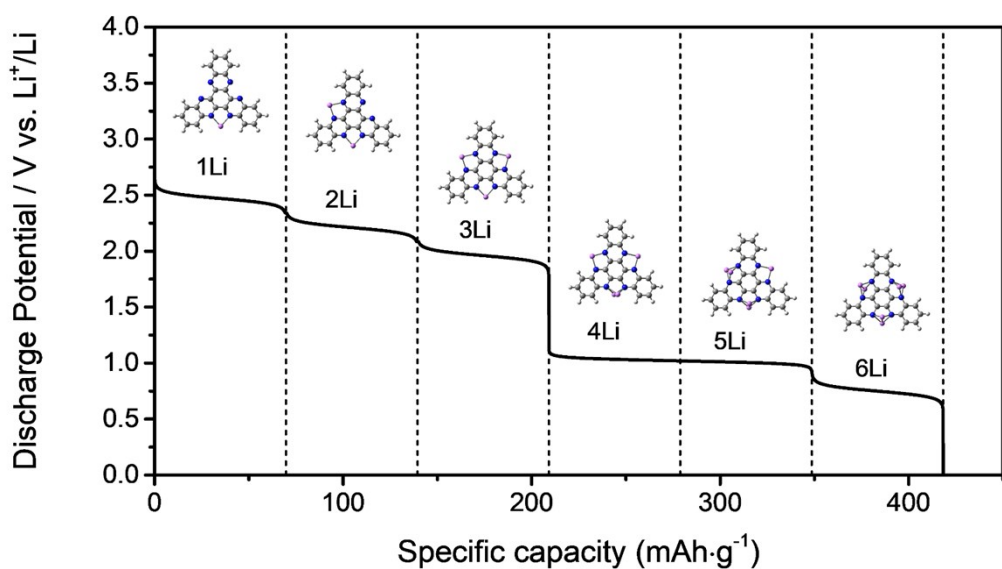


Figure S15. Simulated discharge profiles of TQA.

REFERENCES

1. P. E. Blochl, *Phys. Rev. B*, 1994, **50**, 17953-17979.
2. G. Kresse and J. Furthmuller, *Phys. Rev. B*, 1996, **54**, 11169.
3. G. Kresse and D. P. Joubert, *Phys. Rev. B*, 1999, **59**, 1758-1775.
4. R. Krishnan, J. S. Binkley, R. Seeger and J. A. Pople, *The Journal of Chemical Physics*, 1980, **72**, 650-654.
5. A. D. McLean and G. S. Chandler, *The Journal of Chemical Physics*, 1980, **72**, 5639-5648.
6. C. Lee, W. Yang and R. G. Parr, *Phys Rev B Condens Matter*, 1988, **37**, 785-789.
7. A. D. Becke, *The Journal of Chemical Physics*, 1993, **98**, 5648-5652.
8. G. W. T. M. J. Frisch, H. B. Schlegel, G. E. Scuseria, M. A. Robb, J. R. Cheeseman, G. Scalmani, V. Barone, G. A. Petersson, H. Nakatsuji, X. Li, M. Caricato, A. Marenich, J. Bloino, B. G. Janesko, R. Gomperts, B. Mennucci, H. P. Hratchian, J. V. Ortiz, A. F. Izmaylov, J. L. Sonnenberg, D. Williams-Young, F. Ding, F. Lipparini, F. Egidi, J. Goings, B. Peng, A. Petrone, T. Henderson, D. Ranasinghe, V. G. Zakrzewski, J. Gao, N. Rega, G. Zheng, W. Liang, M. Hada, M. Ehara, K. Toyota, R. Fukuda, J. Hasegawa, M. Ishida, T. Nakajima, Y. Honda, O. Kitao, H. Nakai, T. Vreven, K. Throssell, J. A. Montgomery, Jr., J. E. Peralta, F. Ogliaro, M. Bearpark, J. J. Heyd, E. Brothers, K. N. Kudin, V. N. Staroverov, T. Keith, R. Kobayashi, J. Normand, K. Raghavachari, A. Rendell, J. C. Burant, S. S. Iyengar, J. Tomasi, M. Cossi, J. M. Millam, M. Klene, C. Adamo, R. Cammi, J. W. Ochterski, R. L. Martin, K. Morokuma, O. Farkas, J. B. Foresman, and D. J. Fox, *Revision D.01, Gaussian, Inc., Wallingford, CT*, 2003.
9. M. Yao, H. Senoh, T. Sakai and T. Kiyobayashi, *International Journal of Electrochemical Science*, 2011, **6**, 2905-2911.
10. M. Yao, S.-i. Yamazaki, H. Senoh, T. Sakai and T. Kiyobayashi, *Materials Science and Engineering: B*, 2012, **177**, 483-487.

